

# Augmenter of Liver Regeneration Protein: A Promising Therapeutic Target for Hepatocellular Carcinoma

Sandhya Hora<sup>1</sup>, Savita Mishra<sup>1</sup>, Neha Mathur<sup>2</sup>, Vidhu Aeri<sup>3</sup>,  
Deepshikha Pande Katare<sup>1\*</sup>

<sup>1</sup>Proteomic and Translational Research Laboratory, Centre for Medical Biotechnology, Amity Institute of Biotechnology, Amity University, Noida, Uttar Pradesh, India, <sup>2</sup>Amity Institute of Pharmacy, Amity University, Lucknow, Uttar Pradesh, India, <sup>3</sup>Department of Pharmacognosy and Phytochemistry, School of Pharmaceutical Education and Research, Jamia Hamdard, New Delhi, India

## Abstract

**Background:** Hepatocellular carcinoma (HCC), a deadly cancer form associated with poor prognosis and survival rate represents 5% new patients diagnosed every year worldwide. Despite significant research in the diagnostic, prognostic and therapeutic areas of HCC, no specific validated biomarkers or therapy are available for diagnosis and control the recurrence rate. Augmenter of liver is highly expressed during cirrhosis and has the ability to reduce migration cancerous hepatic cells, hence may have antimetastasis properties. Therefore, it potentiates to become a promising marker for HCC diagnosis as well as the therapeutic target. **Materials and Methods:** Animal model of hepato tumorigenesis was developed using Diethylnitrosamine and 2-Acetylaminofluorene. Biochemical and histopathological examinations were performed to study the disease progression. Furthermore, signature protein was identified using 2 DE gel and matrix-assisted laser desorption/ionization-time-of-flight/mass spectrometry. Docking studies were performed using iGEMDOCK9 for the best binding herbal compound to augmenter of liver regeneration (ALR) for future therapeutic uses. **Results:** Differentially expressed proteins between control and diseased rats were analyzed and one upregulated protein flavin adenine dinucleotide (FAD)-linked sulfhydryl oxidase ALR of 22.8 kDa was found to be present in HCC progression during cirrhosis. **Conclusions:** The present work is a success story with the marker discovery for the prognosis of HCC. This study reports the development of an animal model of liver cancer and systematic screening of protein-based marker FAD-linked Sulfhydryl Oxidase (ALR) with the disease progression. In future, it can be targeted for diagnosis of HCC and therapeutic approach as well.

**Key words:** 2-Acetylaminofluorene, augmenter of liver regeneration, biomarker, diethylnitrosamine, hepatocellular carcinoma, proteomics, Wistar rat model

## INTRODUCTION

Proteomics has revolutionized the way one looks at and deals with proteins. Both the biotechnology and pharmaceutical sciences are being highly impacted by the new window that proteomics has opened.<sup>[1]</sup> This field of study permits the identification, characterization, and quantitation of proteins on a mass scale. Differentially expressed proteins can be developed as biomarkers in a systemic manner and can be used as a tool to decipher the cell function, signaling pathways and disease diagnosis and progression.<sup>[2]</sup>

Hepatocellular carcinoma (HCC) is the fifth lethal cancer and the second common cause of

cancer related mortality in the world.<sup>[3]</sup> More than 7, 00,000 new cases occurring every year of HCC. Liver cancer has a higher prevalence in men than women. In men, it is fifth common cancer (554,000 cases and 7.5% of the total) and ninth in women (228,000 cases, 3.4% of the total).<sup>[4]</sup> HCCs

### Address for correspondence:

Deepshikha Pande Katare, Head Centre for Medical Biotechnology, Room No. 212, Amity Institute of Biotechnology, J-3 Block, Amity University, Sector - 125, Noida - 201 303, Uttar Pradesh, India. Phone: +91-120-4392410. E-mail: dpkatare@amity.edu

**Received:** 17-05-2018

**Revised:** 18-06-2018

**Accepted:** 28-06-2018

are generally diagnosed at advanced stage, so the rate of mortality is the same in men and women both. In this disease, genetic alterations cause transformation of normal hepatocytes into tumor cells.<sup>[5]</sup> Some of the major risk factors for the development of pathology are consumption of alcohol, hepatitis B virus (HBV), hepatitis C virus infection, liver cirrhosis, and carcinogenic agents. Out of the above-mentioned factors, chronic HBV infection is the leading cause of liver carcinogenesis in Asian countries which accounts for 75% cases per annum.<sup>[6,7]</sup>

A wide variety of biomarkers development and drug discovery have been done using the proteomic approach from many years, but only alpha-fetoprotein (AFP) is the only one biomarker for HCC has been developed till date. The specificity and sensitivity of AFP are very low (40–60%), even in some cases of liver injury and in the fatty liver it has found to be increased.<sup>[8-10]</sup> There is a need for early-stage biomarker for diagnosis of HCC to achieve drug targets as well.

The present study reports differentially expressed protein augments of liver regeneration protein (ALRP) during the progression of HCC, would be promising diagnostic biomarker for HCC and can be targeted for therapeutic purpose as cytosolic ALR has antimetastatic and cell migration inhibitory properties.

## MATERIALS AND METHODS

### Animal model of HCC

The liver cancer model was developed by the protocol established by our group previously.<sup>[11]</sup> Animal experiments were accomplished with the ethical standards of the responsible Animal Ethics Committee of Jamia Hamdard (503/CPCSEA).

### Liver function tests

Liver function tests (alanine transaminase [ALT], aspartate transaminase [AST], and alkaline phosphatase [ALP]) were performed using Span kits protocol described by Reitman and Frankel (1957).

### Histopathological examinations

Rats were anesthetized using ether and sacrificed by cervical dislocation. Liver, kidney, brain, stomach, and pancreas were removed out, and 10% buffered formalin was used to fix the tissues.

The tissue slides were formed by hematoxylin and eosin staining and observed for histopathological changes. The images of histopathological slides were taken by utilizing an

Olympus CKX41SF inverted microscope system (Olympus, Japan).

### Sodium dodecyl sulfate-polyacrylamide gel electrophoresis (SDS-PAGE)

SDS-PAGE was carried out using bis-Acrylamide gel (12% resolving and 5% stacking). 10% ammonium persulfate and tetramethylethylenediamine were added for polymerization. Samples were prepared in loading buffer and heating the mixture at boiling water. The sample was loaded into the wells and run using electrophoresis unit set at 100V using Tris-Glycine buffer (1.44% Glycine + 0.3% Tris-base + 0.1% SDS) for 4 h at 100 volts. The gel was immersed in 5 volumes of staining solution for 4 h at room temperature. After 4–5 h, gel was placed in destaining solution after staining to visualize the protein bands.

### Preparation of albumin free sample

#### Column equilibrations

Suspended medium slurry (0.5 ml) was transferred into a spin column and centrifuged at 3,000 rpm for 5–10 s for removing the storage solution. Equilibration buffer (0.3 ml) was added to the medium in the spin column and centrifuged at 3,000 rpm for 5–10 s. This step was repeated twice or thrice.

#### Albumin depletion

Sample (50–100  $\mu$ l) was added to a packed column bed and incubated for 10 min at room temperature. Column was centrifuged for 20 s at 3,000 rpm. Eluate was reapplied to in the collection tube and incubated for 20 s. Unbound proteins were washed off by adding 200  $\mu$ l of equilibration buffer and centrifuged for 20 s at 3,000 rpm. The albumin depleted sample was kept at  $-20^{\circ}\text{C}$ .

#### Two-dimensional (2D) electrophoresis

After separation, identification of proteins in samples has been performed by displacement in 2D oriented at right angles to one another. First, the proteins separation was done on the basis of their isoelectric points. This allows the proteins to resolve independently on the basis of Isoelectric focusing (IEF) and molecular weights over a larger area, increasing the resolution of each component. This is followed by separation on the basis of molecular weight. The specific spot of interest was eluted and trypsinized, and then matrix-assisted laser desorption/ionization-time-of-flight (MALDI-TOF) analysis has been performed to determine the mass of peptides. Before IEF focusing the protein sample was diluted in rehydration buffer such that 125  $\mu$ l will have 50–100 mg protein for 7 cm immobilized pH gradient (IPG) Strip. The sample was loaded the suitable volume. The IPG strips were placed side down slowly from one end to avoid air bubble then the IPG stripes were overlaid with 1.5 ml of mineral oil and left in the

rehydration tray overnight at room temperature. To dehydrate the IPG strips remove the cover from the rehydration tray and blot the tip of the strip on a piece of filter paper to drain mineral oil. Place the focusing tray into the PROTEAN IEF cell and place the equilibration buffer-1 for 10 min and shake. Change the equilibration buffer-2 for 10 min and continue shaking. Perform vertical SDS-PAGE at 150 volts. Stain the gel and destained observe the protein profile.

## Docking studies

### Ligand and protein preparation

Ten flavonoids were identified in 506 food items. The ligands were sketched using 2D-sketcher and later replaced with Maestro workspace. LigPrep2.8 module was used for generating low energy conformations of ligands 16. Similarly, the protein receptor was retrieved from the Protein Data Bank directly in the Protein Preparation Wizard of Maestro9.6 Environment.<sup>[12]</sup> The properties such as molecular weight, octanol/water partition coefficient, brain/blood partition coefficient, Caco-2 cell permeability, HERG K + channel's IC50 values, Human oral absorption, drug-likeness (Lipinski's rule of five), and TPSA were calculated. Docking studies were performed using software iGEMDOCK9 with ALR receptor. Ligands were docked flexibly wherein the conformation generation was limited to variation around asymmetric torsion bonds. Only low energy conformations were kept. The best ligand was chosen according to their Docking Score and Glide Score which are calculated using the standard formula followed by iGEMDOCK9.

## RESULTS

### Morphological changes

Multiple changes were observed in liver morphology during disease progression of Group II in comparison to control liver. Completely faded and nodulated liver were observed in toxin-treated group after 4<sup>th</sup> week of treatment [Figure 1a and b].

### Biochemical tests

#### Liver function tests

##### ALT activity test

ALT activity observed in the control group was 42.19 U/L. ALT activity was seen significantly increased with every repeated dose of toxin. At 1<sup>st</sup>, 2<sup>nd</sup>, 3<sup>rd</sup>, and 4<sup>th</sup> weeks, the increased level of ALT was 72.895, 93.74, 103.625, and 110.055 ( $P < 0.001^{***}$ ), respectively [Figure 2a].

##### AST activity test

The present study shows the increased level in AST levels in comparison to control group. The AST activity was 37.97 in control group and at 1<sup>st</sup>, 2<sup>nd</sup>, 3<sup>rd</sup>, and 4<sup>th</sup> weeks, 63.535

( $P < 0.01^{**}$ ), 87.385, 94.31, and 115.18 ( $P < 0.001^{***}$ ) U/L, respectively [Figure 2b]

##### ALP activity test

The significant increased level was exhibited in ALP activity. In the control group, ALP activity was observed 47.25 U/L. At 1<sup>st</sup>, 2<sup>nd</sup>, 3<sup>rd</sup>, and 4<sup>th</sup> weeks, ALP level was 77.215 ( $P < 0.01^{**}$ ), 89.41, 91.23, and 110.435 U/L ( $P < 0.001^{***}$ ) [Figure 2c].

### Antioxidant assays

#### Total glutathione (GSH)

Total GSH level of control group was 2.45  $\mu$ mole/g tissue/h and at 1<sup>st</sup>, 2<sup>nd</sup>, 3<sup>rd</sup>, and 4<sup>th</sup> weeks 1.785, 1.56, 1.155, and 1.065  $\mu$ mole/g tissue/h. In the present paper, significant decrease observed in GSH level [Figure 3a].

#### Lipid peroxidation

Malondialdehyde (MDA) level of control group was 2.416 nmol of MDA formed/h/mg tissue. At 60<sup>th</sup> and 150<sup>th</sup> days, MDA content

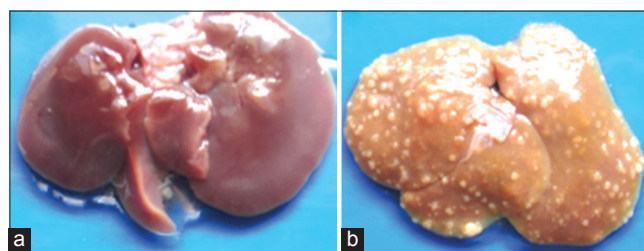


**Figure 1:** Morphological changes in control and diseased liver. (a) Control, (b) Diseased

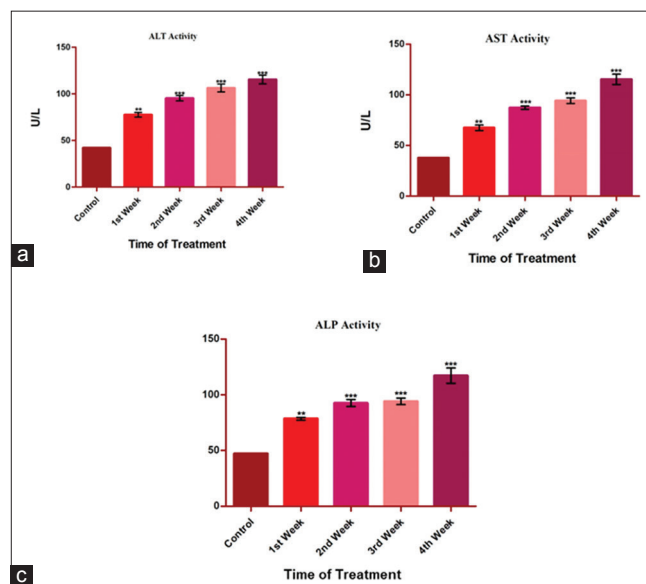


**Figure 2:** Biochemical analysis of liver function tests from serum. Alanine transaminase (a) aspartate transaminase (b) and alkaline phosphatase (c) were performed from serum after 1<sup>st</sup>, 2<sup>nd</sup>, 3<sup>rd</sup>, and 4<sup>th</sup> toxin treatment of the animals of both groups (\* $<0.05$ ; \*\* $<0.01$ ; \*\*\* $<0.001$ )

was seen to be 2.462 and 3.077 ( $P < 0.001^{***}$ ) nmol formed/h/mg tissue, respectively, in the treated group [Figure 3b].

### Catalase activity

The catalase activity was exhibited to be decreased significantly in the toxin-treated animal as a comparison to control animals. The catalase activity of control subjects was 0.91 U/mg. At 1<sup>st</sup>, 2<sup>nd</sup>, 3<sup>rd</sup>, and 4<sup>th</sup> weeks, the catalase activity of toxin-treated group animals was 0.71 ( $P < 0.05^*$ ), 0.545 ( $P < 0.01^{**}$ ), 0.39 ( $P < 0.001^{***}$ ), and 0.26 U/mg ( $P < 0.001^{***}$ ), respectively [Figure 3c].

### Histopathological analysis

The histopathological analysis was done in the liver tissue of the control and toxin-treated group. Tissue samples of control group showed normal architecture without any degeneration or necrosis. Normal hepatocytes were seen in cord pattern with a portal triad (PT) and central vein (CV) [Figure 4a and c]. Tissue sample of toxin-treated group showed centrilobular necrosis and sinusoidal dilation around the CV area in low power photomicrograph and high power photomicrograph from the same section showing a portion of a hepatocytic nodule showed atypical features such as anisonucleosis, prominent nucleoli, and presence of very large nuclear profiles [Figure 4b and d].

### One dimensional (1D) and 2D electrophoresis

1D and 2D electrophoresis were done for serum samples. We have observed many differentially expressed proteins in 1D protein profiling [Figure 5a]. 2D PAGE was done for 3 weeks alternatively after toxin treatment. Significant changes were observed in 2DE protein profiling after 3 weeks of toxin challenge [Figure 5b]. We have taken few proteins to be validated for a prospective biomarker for HCC.

### MALDI-TOF-mass spectrometry (MS/MS)

Differentially expressed proteins were further characterized by MALDI-TOF-MS/MS. Data were analyzed using Mascot (www.matrixscience.com) search engine. NCBIprot database was used to search protein sequences and confirmation the genus (*Rattus*) [Figure 6a and b]. We have also extracted three-dimensional (3D) structure of ALR from PDB database [Figure 6c]. We have picked upregulated spot-28 of low molecular weight protein as a prospective prognostic biomarker for HCC as it is present at early weeks of disease progression in continuity. Peptide sequence was searched in Mascot search engine, and we have found flavin adenine dinucleotide (FAD)-linked sulfhydryl oxidase ALR (Molecular Mass-22837) [Figure 6c].

Database: NCBIprot 20171205 (139213787 sequences; 51013024959 residues)

Taxonomy: *Rattus* (85708 sequences)

Timestamp: 3 Dec 2017 at 06:05:48 GMT

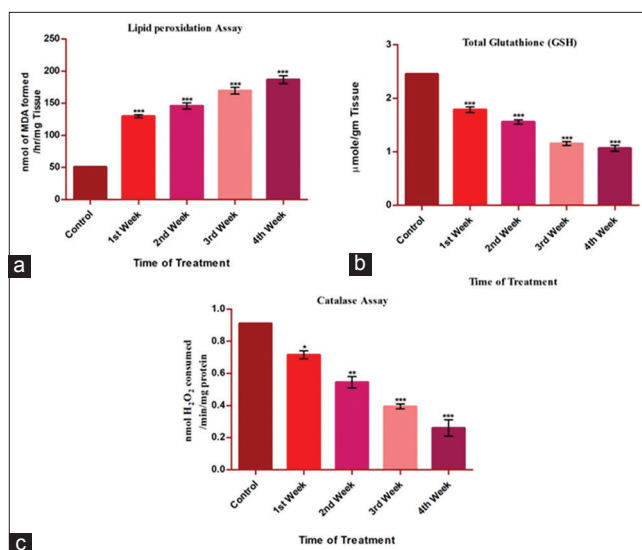


**Figure 3:** Biochemical analysis of antioxidant assays from the tissue. Lipid peroxidation (a), glutathione (GSH) (b), and catalase (c) were performed of the subjects from both groups to observe the oxidative stress in liver tissue with the progression of disease. Malondialdehyde level is increased and reduced GSH activity, catalase activity is significantly decreased. (\* $<0.05$ , \*\* $<0.01$ ; \*\*\* $<0.001$ )

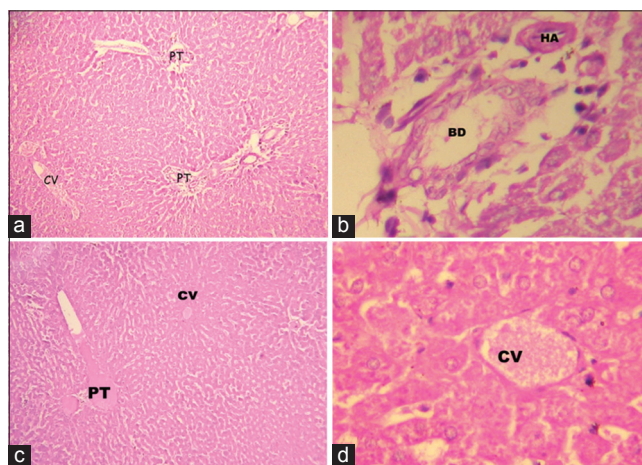


**Figure 4:** Histopathological studies (a) low power photomicrograph of liver section from control group animal showing normal hepatic parenchyma. (H and E,  $\times 100$ ). (b) High power photomicrograph of section of liver from Control Group animal showing a normal portal triad with bile duct and hepatic artery (H and E,  $\times 400$ ). (c) Low power photomicrograph of liver section from Diethylnitrosamine + 2-acetylaminofluorene (2-AAF) treated group showing hepatic parenchyma with disruption in normal architecture. Nodules of regenerating hepatocytes separated by thin septae are present. There is inflammatory cell infiltration around the portal triads (H and E,  $\times 100$ ). (d) High power photomicrograph of section of liver from AAF treated group showing the presence of numerous red blood cell clusters in the sinusoids (H and E,  $\times 400$ )

Top score: 89 for NP\_037354.2, FAD-linked sulfhydryl oxidase ALR [*Rattusnorvegicus*]

Protein sequence coverage: 33%

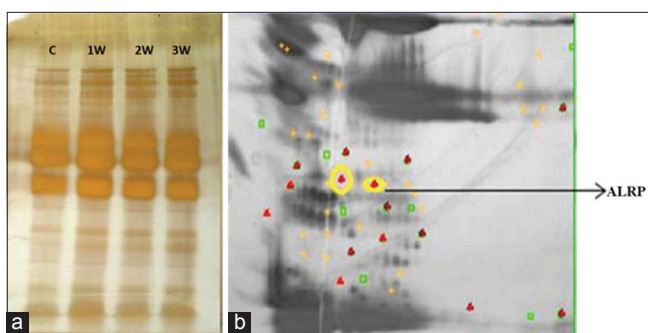


**Figure 5:** Sodium dodecyl sulfate-polyacrylamide gel electrophoresis analysis. (a) 1D electrophoresis showing differentially expressed proteins in Lane 1-control, Lane 2-1<sup>st</sup> Week, Lane 3-2<sup>nd</sup> Week, and Lane 3-3<sup>rd</sup> Week. (b) 2D electrophoresis with PD quest analysis showing differentially expressed protein spots

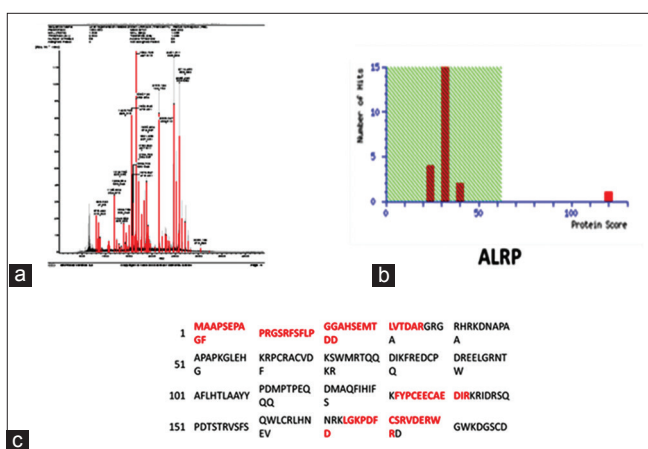


**Figure 6:** (a) Chromatogram of augmenter of liver regeneration (ALR) and (b) histogram showing a probability based MOWSE score of ALR. MOWSE Score is 89 (>62,  $P < 0.05$ ) (c) mass spectrometry (MS)/MS peptide summary of ALR (matched peptide shown in bold red)

Protein scores >62 are significant ( $P < 0.05$ ).

### Docking studies

Among 10 ligands Bleomycin showed highest binding energy (-119.412). It was found that DB00290 (Bleomycin) has the best efficacy for the ALR [Table 1]. 3D structure of ALR and best-docked image of ALR with bleomycin has been showed in Figure 7a and b.

## DISCUSSION

HCC is second-ranked cancer worldwide. There are not much diagnostic or prognostic markers are available for its treatment.<sup>[3,4]</sup> To date only AFP is the protein that has been widely studied and used for the diagnostic purpose.<sup>[13]</sup> The conventional methods available for diagnosis and the treatment of HCC are not very effective. Hence, it should be accompanied with the

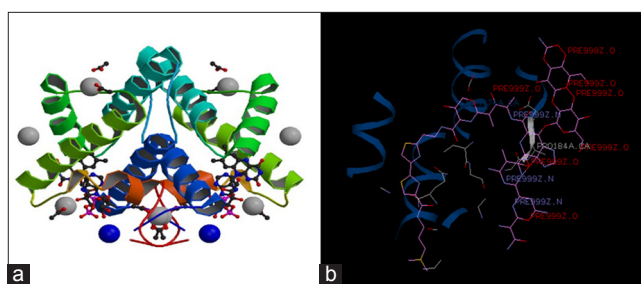


**Figure 7:** (a) Three-dimensional structure of augmenter of liver regeneration (ALR) extracted by www.rcsb.org. (b) Best docked pose of ALR with bleomycin

accumulation of cancer-related genes, so that it can measure by genetic analysis. The differentially expressed proteins involved in HCC can provide the directions of the multi-step process of HCC and can be used to elucidate the molecular mechanism involved in multifarious clinical features.<sup>[14]</sup>

The level of liver function enzyme has been elevated during HCC progression, similarly, Ghuman and Gowda reported in cirrhosis and HCC condition. We have observed significant increased level in ALT and AST with the progression of the disease as reported in earlier reports.<sup>[15]</sup> The present study supported by histopathological observations regarding HCC. Schlageter *et al.* showed the histopathological analysis of hepatocarcinogenesis, in accordance with this study, present work also depicts the hepatic parenchyma with disruption in normal architecture and nodules of regenerated hepatocytes separated by thin septae are present.<sup>[16]</sup> Several red blood cell (RBC) clusters and PT surrounded by cell infiltration have also been observed in disease progression.<sup>[17]</sup>

Cell infiltration around portal triads and the presence of numerous RBC clusters in the sinusoids also has been observed, and early toxicity of disease is supported by histopathological observations in liver.<sup>[18]</sup> ALR, human augmenter of liver involves in catalyzing disulfide bond formation and also play a role in cell survival through its CXXC motif. It also potentiates antimetastatic activity in liver cancer. According to literature, the enhanced level of ALR has been observed in cirrhotic patients, similarly, we have also observed its high expression from cirrhosis to HCC.<sup>[19]</sup>

In the present study, protein profiles were compared between control and HCC serum using proteomic approach. 2D profile of the sample diethylnitrosamine + 2-acetylaminofluorene (200 mg/kgBW) showed corresponding changes in the same regions. Vedarethinam *et al.* showed proteomic analysis for HCC in their study, in accordance with this we also found some upregulated and some downregulated proteins in our work.<sup>[20]</sup>

## CONCLUSIONS

In the present study, the most prominent upregulated protein at early weeks of HCC progression was characterized by

**Table 1:** Binding energies of ligands bind to ALR

Ligand	Total energy	VDW	H Bond	Elec	AverConPair
Bleomycin.pdb	-119.412	-97.2139	-22.1981	0	8.35417
Vincristine.pdb	-116.1	-94.7139	-21.386	0	12.9833
Mitocin.pdb	-109.327	-72.1108	-37.2157	0	28.625
Teniposide.pdb	-101.662	-81.6001	-20.0624	0	13.0652
Quercetin.pdb	-99.2914	-81.4732	-17.8181	0	27.3636
Perthexiline1.pdb	-99.1844	-92.1844	-7	0	28.05
Silvestrol-1.pdb	-93.8148	-84.3148	-9.5	0	25.95
Flovopirridol-0.pdb	-84.5193	-68.0421	-16.4772	0	16.3571
Berberin-0.pdb	-82.4977	-70.5027	-11.995	0	21.28
Vinorelbine-0.pdb	-118.128	-128.44	-7.31193	0	6.92982

ALR: Augmenter of liver regeneration

mass spectroscopy, i.e., FAD-linked Sulfhydryl Oxidase Protein (ALRP). Augmenter of ALR is highly expressed in cirrhotic hepatocytes and HCC malignancies. In conclusion of this study, it is to be suggested that FAD-linked Sulfhydryl Oxidase (ALRP) can be targeted in the future for drug delivery to diagnose HCC at cirrhosis or metastasis stage. Docking studies exhibit the highest efficacy of ALR with Bleomycin; hence, the present study predicts that ALR can be targeted by Bleomycin during cirrhosis or metastatic phase.

## ACKNOWLEDGMENTS

We gratefully acknowledge founder president Dr. Ashok Chauhan, Amity University, Uttar Pradesh, Noida, for providing infrastructure.

## REFERENCES

- Megger DA, Naboulsi W, Meyer HE, Sitek B. Proteome analyses of hepatocellular carcinoma. *J Clin Transl Hepatol* 2014;2:23-30.
- Lee SC, Tan HT, Chung MC. Biomarkers for recurrence of hepatocellular carcinoma. *Biomark Liver Dis* 2017;167-91.
- Torre LA, Bray F, Siegel RL, Ferlay J, Lortet-Tieulent J, Jemal A, *et al.* Global cancer statistics, 2012. *CA Cancer J Clin* 2015;65:87-108.
- Wanich N, Vilaichone RK, Chotivitayatarakorn P, Siramolpiwat S. High prevalence of hepatocellular carcinoma in patients with chronic hepatitis B infection in Thailand. *Asian Pac J Cancer Prev* 2016;17:2857-60.
- Jovel J, Lin Z, O'keefe S, Willows S, Wang W, Zhang G, *et al.* Novel insights into the molecular heterogeneity of hepatocellular carcinoma. *BioRxiv* 2017;2017:101766.
- Corey KE, Gawrieh S, deLemos AS, Zheng H, Scanga AE, Haglund JW, *et al.* Risk factors for hepatocellular carcinoma in cirrhosis due to nonalcoholic fatty liver disease: A multicenter, case-control study. *World J Hepatol* 2017;9:385-90.
- Global Burden of Disease Liver Cancer Collaboration, Akinyemiju T, Abera S, Ahmed M, Alam N, Alemayohu MA, *et al.* The burden of primary liver cancer and underlying etiologies from 1990 to 2015 at the global, regional, and national level: Results from the global burden of disease study 2015. *JAMA Oncol* 2017;3:1683-91.
- Mao L, Wang Y, Wang D, Han G, Fu S, Wang J, *et al.* TEMs but not DKK1 could serve as complementary biomarkers for AFP in diagnosing AFP-negative hepatocellular carcinoma. *PLoS One* 2017;12:e0183880.
- Ge T, Shen Q, Wang N, Zhang Y, Ge Z, Chu W, *et al.* Diagnostic values of alpha-fetoprotein, dickkopf-1, and osteopontin for hepatocellular carcinoma. *Med Oncol* 2015;32:59.
- Witjes CD, van Aalten SM, Steyerberg EW, Borsboom GJ, de Man RA, Verhoef C, *et al.* Recently introduced biomarkers for screening of hepatocellular carcinoma: A systematic review and meta-analysis. *Hepatol Int* 2013;7:59-64.
- Malik S, Bhatnagar S, Chaudhary N, Katare DP, Jain SK. DEN+2-AAF-induced multistep hepato tumorigenesis in wistar rats: Supportive evidence and insights. *Protoplasma* 2013;250:175-83.
- Hsu KC, Chen YF, Lin SR, Yang JM. IGEMDOCK: A graphical environment of enhancing GEMDOCK using pharmacological interactions and post-screening analysis. *BMC Bioinformatics* 2011;12 Suppl 1:S33.
- Bruix J, Reig M, Sherman M. Evidence-based diagnosis, staging, and treatment of patients with hepatocellular carcinoma. *Gastroenterology* 2016;150:835-53.
- Attwa MH, El-Etreby SA. Guide for diagnosis and treatment of hepatocellular carcinoma. *World J Hepatol* 2015;7:1632-51.
- Deterding K, Höner Zu Siederdisen C, Port K, Solbach P, Sollik L, Kirschner J, *et al.* Improvement of liver function parameters in advanced HCV-associated liver cirrhosis by IFN-free antiviral therapies. *Aliment Pharmacol Ther* 2015;42:889-901.

16. Schlageter M, Terracciano LM, D'Angelo S, Sorrentino P. Histopathology of hepatocellular carcinoma. *World J Gastroenterol* 2014;20:15955-64.
17. Tsurusaki M, Sofue K, Isoda H, Okada M, Kitajima K, Murakami T. Comparison of gadoxetic acid-enhanced magnetic resonance imaging and contrast-enhanced computed tomography with histopathological examinations for the identification of hepatocellular carcinoma: A multicenter phase III study. *J Gastroenterol* 2016;51:71-9.
18. Huang Y, Zhou S, Zhu J, Lubman DM, Mechref Y. LC-MS/MS isomeric profiling of permethylated N-glycans derived from serum haptoglobin of hepatocellular carcinoma (HCC) and cirrhotic patients. *Electrophoresis* 2017;38:2160-7.
19. Dayoub R, Wagner H, Bataille F, Stöltzing O, Spruss T, Buechler C, *et al.* Liver regeneration associated protein (ALR) exhibits antimetastatic potential in hepatocellular carcinoma. *Mol Med* 2011;17:221-8.
20. Vedarethinam V, Dhanaraj K, Soundherrajan I, Sivanesan R. Identification of differential protein expression in hepatocellular carcinoma induced wistar albino rats by 2D electrophoresis and MALDI-TOF-MS analysis. *Indian J Clin Biochem* 2016;31:194-202.

**Source of Support:** Nil. **Conflict of Interest:** None declared.